

Replication of micro-structured surfaces by integrating AM with PIM

Alberto Basso¹, Simon Emil Christensen¹, Macarena Méndez Ribó¹, Peter Kjeldsteen², Peter Valler², David Bue Pedersen¹, Yang Zhang¹

¹Technical University of Denmark, Department of Mechanical Engineering, Denmark

²Sintex A/S, Denmark

albass@mek.dtu.dk

Abstract

3DIMS, 3D-Printing Integrating Manufacturing System, is a process that couples additive manufacturing (AM) with powder injection moulding (PIM). This process allows overcoming some limitations of the conventional injection moulding process such as: high tooling cost, geometrical constraints and failure to manufacture customized parts. This novel process chain works as follows: a sacrificial thin wall mould is fabricated with a vat-photopolymerisation AM machine, successively the mould is filled with a feedstock made of metal powder and a multi binder system, after that the mould is dissolved and the part is debound and sintered. This work presents a description of the manufacturing chain focusing on the geometrical deviation for each step of the process. The quality of the replication is evaluated by investigating the geometrical displacement of micro-features on the surface, using an Olympus Lext confocal microscope and computed tomography.

Powder Injection Moulding, Additive Manufacturing, Soft tooling, Sacrificial mould, Fingerprint

1. Introduction

A well-known technology for mass production of metal parts is Powder Injection Moulding (PIM). This technology is more cost effective than machining [1], but expensive when dealing with prototyping or low rate manufacturing. The metal tools for the injection moulding machine are cost effective only when parts are mass produced. Another problem of PIM is the production of intricate geometries, which can be achieved only by using complex mould (thus expensive), or not achievable when features like twisted inner channels are present.

In order to achieve complex geometries, Charter et al. [2] and Zhang et al. [3] proposed to use a sacrificial core, nonetheless, this process requires additional step for the core removal. Hein et al. [4] suggested using a sacrificial mould thermally degraded after the injection process. The process proposed by Hein gives freedom in designing the mould solving the issue of producing parts with complex geometries, however, thermal degradation of the mould generates deformations on the final part.

Lately, several researchers have investigated the use of soft tooling in the injection moulding process [5-8]. Soft tooling in injection moulding aims to lower the cost of the mould fabrication [5], making PIM feasible even for prototyping and low rate manufacturing.

In this work an innovative process that hybridize Additive Manufacturing (AM), with PIM is used: 3DIMS, 3D-Print Integrating Manufacturing System. This process uses a sacrificial mould produced by vat polymerization based additive manufacturing (VPAM) that can be chemically dissolved in a water-based solution. The mould is mounted in an injection moulding machine, filled with a specifically developed feedstock, ejected and then dissolved. After the mould dissolution, i.e. the part ejection process, the ejected part is debound and sintered. Using a water-soluble sacrificial mould

as tool for PIM allows to achieve complex geometries and reduce the tooling cost, making this process convenient when dealing with the production of highly customized parts, pilot production and low rate manufacturing.

Lately there is an increasing interest in the production of micro structured surfaces, found in different fields such as optics and energy [9]. Here arrays of micro pyramids are used as fingerprint. A fingerprint is a physical product feature, i.e. micro pillars and micro holes, that does not prevent the functionality of the component [10]. The quality of the fingerprint has been found to be correlated with the overall quality of the part as shown by Calaon et al. in [11] and Giannakas et al. in [12]. The fingerprint concept is thus used to validate the geometrical stability of the part during the production steps.

The use of a closed sacrificial mould creates challenges when measuring these kind of geometries. It is not possible to evaluate the dimensions of the cavity and inner structures of the mould with the conventional optical and tactile methods without damaging the insert itself. In this work both optical microscopy and computed tomography (CT) are used, and the replication of microstructures is investigated in different process steps. Knowing the variation in dimension of the part during each process step, highlights which manufacturing process step needs improvement. In the case where there is no room for improvement in a specific step, knowing when and where the variation will occur allows to compensate the geometrical displacement during the designing phase.

2. Materials and methods

2.1. 3DIMS process The 3DIMS process, depicted in Figure 1, couples additive manufacturing with injection moulding. The

mould, or insert, is fabricated via vat polymerization using a Peopoly Moai SLA printer. Vat polymerization is an additive manufacturing technique where a photopolymer, or a light-activated liquid resin, is cured when it is exposed to UV-light. In

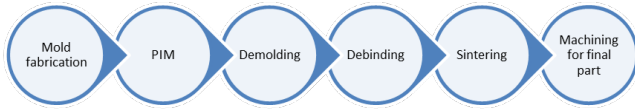


Figure 1: The 3DIMS process chain.

the present process chain, a water-soluble photopolymer is used, allowing to dissolve the mould in an alkaline solution. The photopolymer used is IM 2.0 produced by Addifab. After the production of the mould, hereafter called insert, the additive manufactured insert is positioned inside a metal mould in an injection moulding machine. The injection moulding machine used is a Nissei THM7, the feedstock is melted at a temperature of 90°C and the mould temperature is set at room temperature (23°C). Since the injection is done into a polymeric insert with thin walls, the feedstock injection pressure needs to be relatively low, specifically 20 bar, to avoid distortion of the 3D printed mould during the injection. In order to use low injection pressure a new feedstock for PIM processes was developed. The used feedstock has a solid loading of 60% in 316L stainless steel and a specifically designed binder system with low viscosity. After the injection, the filled insert is removed from the mould. The conventional ejection of the part is not carried out in the injection moulding machine but in an additional step: the mould dissolution. The printed insert, filled with the metal feedstock, is dissolved in an alkaline solution. The binder system of the feedstock was designed to withstand the dissolution process without causing any geometrical distortion of the part. Once the insert is dissolved, the green body is obtained. At this stage, the binder system needs to be removed from the green body. i.e. debinding. The debinding process is done in two steps: chemically and thermally. First, the green body is treated chemically in n-heptane for 24 hours at 50°C, and then is thermally treated with the heating cycle described in Table 1. After is sintered at 1360°C in a protective atmosphere to avoid oxidation.

Table 1: Heating cycle of the thermal debinding process.

Temperature	Heating rate	Time [h]
20°C → 230°C	2°C/min	1:45
230°C → 230°C	hold	1
230°C → 500°C	1°C/min	4:30
500°C → 500°C	hold	3
500°C → 20°C	-	-

2.2. Sample design

Two different set of features are used in two different moulds. The investigation of the geometrical dimension of the mould via optical microscopy and CT is done using moulds with micro pyramids, referred as pyramid insert; the degree of replication is investigated using an insert with square tapered pillars and holes, hereinafter called square insert.

Since the microstructures are located on the inner surfaces of the mould, it is not possible to measure directly the dimensions of the pyramids with optical microscopy without ruining the insert itself. In order to overcome this problem, two open moulds were printed together with the closed insert for every

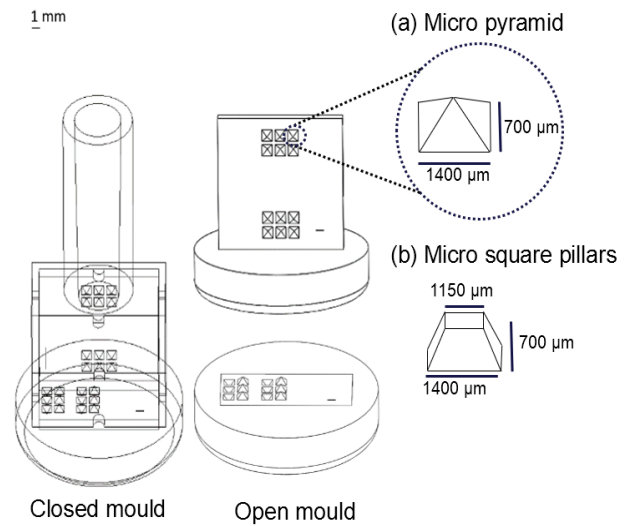


Figure 2: Closed mould with pyramid structure on the left, two open moulds for optical measurements on the right. Another version with micro square pillars was also created to study the degree of replication in the process chain.

printed batch. Figure 2 , on the left, shows the design for the closed insert. The cylindrical part of the insert is the sprue with the injection gate location. Two groups of six micro pyramids with nominal height of 700 µm each are presented on both the vertical wall and on the bottom, in each group three pyramids are pointing out (outwards pyramids) and three in (inwards pyramids). The square insert has the same overall mould configuration as the previously described pyramid insert. Figure 2 (b) shows a detail of the design of the square insert. Six square pillars and six square holes with height and depth of 700 µm were designed on the vertical wall and bottom part of the cavity in the insert.

3. Measurements

3.1 Deviation from optical microscopy to CT

As aforementioned, it is not possible to measure directly the dimensions of the micro features on the closed insert with optical microscopy. Therefore, CT is used to investigate height and width of the microstructures without damaging the mould. In this section the height of the micro pyramids of the open inserts in Figure 2 were first measured with a Werth CT-scan (pixel size of 51 µm), and then measured again with an Olympus LEXT 4100 confocal laser-scanning microscope. This investigation is done in order to identify the best characterization method to evaluate the geometrical deviation in the process chain.

Figure 3, shows the variation of the height and depth of micro pyramids on the bottom and on the vertical wall. The dimensions of inwards and outwards pyramids seem to be more stable for the microstructure printed on the bottom of the insert. The standard deviation of the height of the inwards pyramids on the bottom is 11 µm, while the one for the pyramids on the vertical wall is 35 µm, similar deviations are found for the outwards pyramids. The structures on the bottom are parallel to the printing layer, meaning that the accuracy of the printing depends on the motor of the building plate (resolution of 25 µm on z-direction). On the other hand, the micro pyramids on the wall are perpendicular to the printing direction. In this case, the resolution of the printer depends on the laser (resolution on the xy-direction is 70 µm), which is lower than the resolution of the motor.

Looking now at the height of the pyramids, it is noticeable how, for both bottom and wall, the height of the inwards pyramids is closer to the nominal value of 700 μm . The height of outwards pyramids, instead, deviated from the nominated value largely because the tip part could not be printed; it is relative easy to print a hole with a sharp tip than to print a pillar. This is particularly true for the outwards pyramids in the bottom.

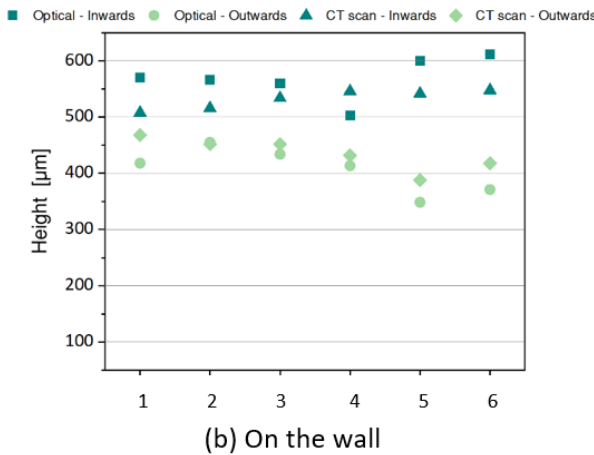
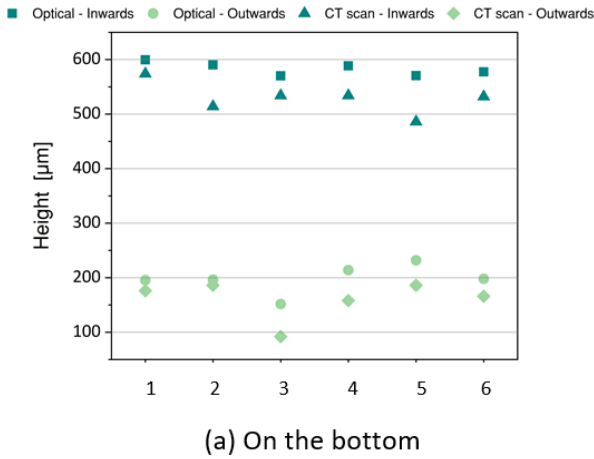


Figure 3: Height and depth of the micro pyramids measured with the optical microscope and CT scan for both inwards and outwards pyramids on the bottom and on the wall.

Looking at the difference between CT and optical microscope in Figure 3, it is noticeable that in almost all the cases the value of the height measured through optical method is higher, the only exception is for the outwards pyramids on the wall. The resolution of the optical microscope on the z-direction is 10 nm and the CT pixel size is 51 μm . The variation between the height value calculated with the optical microscope and CT is approximately 10%. The measurement uncertainty was estimated taking both machine error and process into account, using the following equation:

$$U = k \cdot \sqrt{u_m^2 + u_p^2} \quad (1)$$

The uncertainty of the height measured with the optical microscope is 8.1 μm . The results between CT scan and optical microscope are quite similar, however, considering the higher resolution of the optical microscope, time needed to carry out the investigation and equipment availability, it was decided to investigate the dimensions of the micro features using optical microscopy.

3.2 Deviation from open to close mould

In order to investigate the microstructures with the optical microscope without damaging the insert, the optical measurements were done on the open moulds depicted in Figure 2. The open moulds are used as measurement artefacts and is necessary to evaluate the deviation from open to closed mould to quantify a potential source of error. After a mould is manufactured, it requires an additional UV-curing step, to finalize crosslinking. The microstructures on the closed mould are situated in the inner surfaces, thus they are subjected to fewer irradiation to UV-light in comparison to the microstructures on the open moulds. The higher the degree of curing the higher is the shrinkage [13]. This phenomenon can

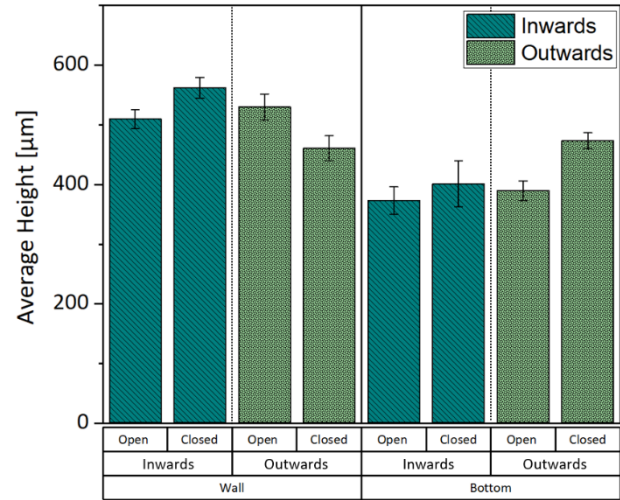


Figure 4: Average height of micro pyramids on the wall and bottom in the open and closed mould respectively. Error bars indicate the standard deviation of the height calculate from six pyramids.

cause deviation between open and closed mould. The evaluation of the deviation is done by measuring the height of the micro pyramids of a closed insert that was cut and measured with the optical microscope and the equivalent microstructures on the two open moulds.

Figure 4 depicts the average height of the microstructures in open and closed moulds for bottom and vertical walls. The overall deviations do not follow a noticeable trend; thus, it is not possible to make any assumptions about the error generated by using open mould as a measurement artefact. However, taking into account the measurements uncertainty and the repeatability of the pillars, the deviation between open and closed mould can be considered small. Hence, the open mould can be used as measurement artefact to evaluate the dimension of the features in the closed insert.

4. Replication rate in the process chain

The validation of the fingerprint concept is carried out by correlating the overall height and width of the moulded part with the dimensions of the microstructures. The overall dimension of the printed inserts and moulded parts were measured with a CMC DeMeet 220 (maximum permissible error 4.1 μm). This study was done using the square insert (Figure 2b), measuring height and width of pillars and holes in the bottom and vertical wall of the mould, and their respectively negative structure on the part (i.e. a pillar on the mould is a hole in the part).

The bar chart in Figure 5 (a) depicts the degree of replication of the height of the microstructures and the overall height of the part during two consecutive steps of the process chain:

debinding and sintering. The precedent step, i.e. demoulding, is not possible to assess because the paraffin wax present in the injected slurry settles over the surface veiling the features. The degree of replication is calculated as follow:

$$\text{Degree of replication} = \frac{\text{Dimension on the part}}{\text{Dimension on the mould}} \quad (2)$$

From Figure 5 (a) is possible to see how the degree of the replication of the height of the mould pillars (i.e. holes in the part) does not match the replication of the overall height of the part after debinding. Considering the low strength of the mould material, the pillars in the mould might be compressed by the pressure during the injection of the feedstock, explaining the low degree of replication for such features after the debinding step. After sintering, the pillars on the mould (holes in the part) have similar degree of replication to the overall height of the part. Nonetheless, since it was not possible to find a correlation between height of microstructure and overall height of the part during the debinding step, the fingerprint concept as quality indicator for the process chain cannot be validated.

On the other hand, the graph in Figure 5 (b) shows similar degree of replication between the width of the microstructure and the overall width of the part for both debinding and sintering. It is thus possible to use the fingerprint concept to correlate the overall quality of the part by investigating the width of the microstructures.

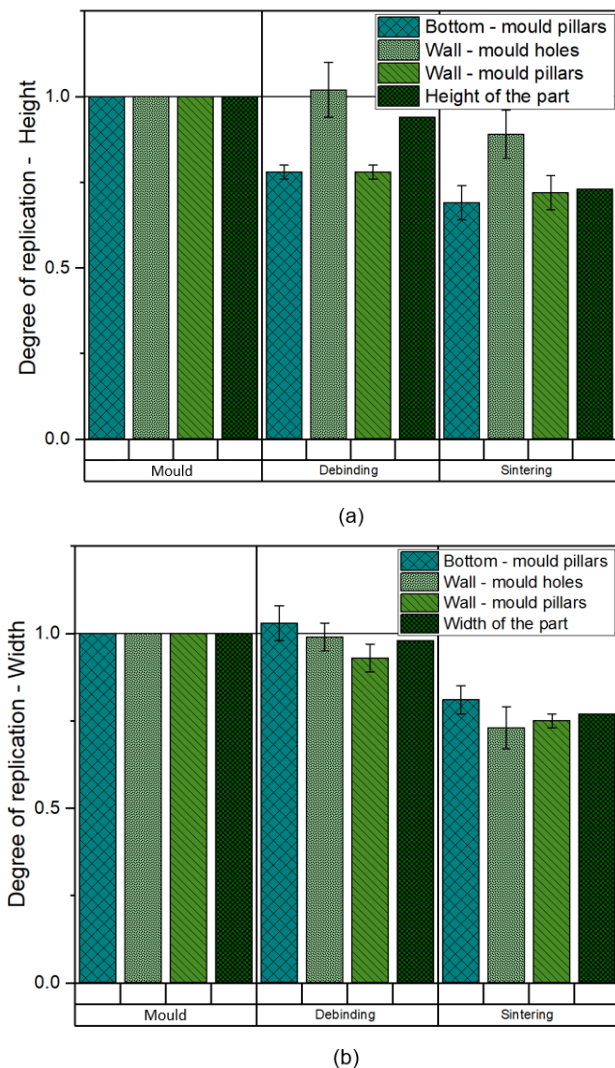


Figure 5: Replication rate in the process chain of: height of the overall part and height of microstructure in (a), and overall width of the part and width of the microstructure in (b).

5. Conclusion

This work describes a novel process chain for metal powder injection moulding (PIM), which is particularly valuable for prototyping and manufacturing of highly customized part with complex structures.

Both optical microscopy and computed tomography (CT) were investigated in order to identify a possible characterization method for the process chain. Considering the measurements uncertainty, time needed to carry out the investigation and accessibility to the equipment, optical microscopy was identified as the most suitable tool to evaluate the geometrical displacement in the production steps.

This paper has also evaluated the use of open moulds as measuring artefacts to study the dimensions of micro features in the closed mould. The investigation showed small deviation in the value of the height between the microstructures in the open and closed mould, allowing the use of the open moulds as measuring artefact.

The final aim of this paper was to validate the fingerprint concept as quality indicator throughout the process chain. It was demonstrated that by solely measuring the width of the microstructures the geometrical stability of the whole part can be validated quantitatively after debinding and sintering.

Acknowledgement

The work has been supported by Innovation Fund Denmark through the project "3DIMS – 3D-Printing Integrated Manufacturing System" (Grant no. 6151-00005A).

References

- [1] Atre S V, Weaver T J, and German R M. 2010 *SAE Technical Paper Series*.
- [2] Chartier, T., Delhomme, E., Baumard, J. -F., Veltl, G., & Ducloux, F., 2001. Injection Moulding of Hollow Silicon Nitride Parts Using Fusible Alloy Cores. *Ceram Int*, **27** (7): 821–27.
- [3] Zhang, S. -X., Ong, Z. Y., Li, T., Li, Q. F., & Ng, F. -L., 2010. Feasibility Study on Producing Components with Embedded Channel by Powder Injection Moulding, *Key Eng Mater*, **447**: 401–5.
- [4] Hein SB. 2018, Lost-Form Powder Injection Moulding - Combining Additive Manufacturing and PIM, *Euro PM 2018-PIM processing*.
- [5] Tosello G, Charalambis A, Kerbache L, Mischkot M, Bue Pedersen D, Caloan M and Nørgaard Hansen H. 2019 *The Int. J. of Advanced Manufacturing Technology*. **100** 783-795.
- [6] Zhang Y. Bue Pedersen D, Mischkot M, Caloan M, Baruffi F and Tosello G 2018 *J. of Visualized Experiment* . **138**.
- [7] Zhang Y. Bue Pedersen D, Segebrecht Gøtje A and Mischkot M 2017 *J. of Manufacturing Processes*. **27** 138-144.
- [8] Mischkot M, Nørgaard Hansen H and Bue Pedersen D 2015 *Proceedings of Euspen's 15th International Conference & Exhibitions*.
- [9] Zhang S, Zhou Y, Zhang H, Xiong Z, To S. 2019 Advances in ultra-precision machining of micro-structured functional surfaces and their typical applications, *Int.J. of Machine Tools and Manufacture*. **142**, 16-41.
- [10] Giannikas, N. 2018 Precision Injection moulding of micro features using integrated process and product quality assurance. *PhD Thesis*. 21-36.
- [11] Caloan, M, Hansen, H. -N, Tosello, G., Garnæs, J, Nørregaard, J, & Li, W. 2015, Microfluidic chip designs process optimization and dimensional quality control, *Mirosyst Technol*, **21**(3), 561–570.
- [12] Giannikas, N, Kristiansen, PM, Zhang, Y, & Tosello, G. 2018, Investigation of product and process fingerprints for fast quality assurance in injection molding of micro-structured components. *Micromachines*, **9**(12), 661.
- [13] Silikas N, Eliades G, and Watts DC, 2000, Light intensity effects on resin-composite degree of conversion and shrinkage strain, *Dental Materials* **16**, 292-296.